Adsorption of hazardous crystal violet dye by almond shells and determination of optimum process conditions by Taguchi method

Ali Goksu*, Mehmet Kayra Tanaydin

Munzur University, Faculty of Engineering, Department of Chemical Engineering, 62000, Tunceli, Turkey,
Tel. +90 428 213 1794-1815, email: aligoksu58@hotmail.com (A. Goksu), tanaydinmehmet@gmail.com (M.K. Tanaydin)

ABSTRACT

Almond shells are classified as an agricultural waste of the food industry. In this study, almond shells were prepared as efficient adsorbents for removing Crystal Violet (CV) dye. The effects of adsorbent dosage, pH, initial concentration, shaking speed, temperature and particle size were studied. The Taguchi L25 experimental design method was used to obtain the optimum experimental condition. The data were analyzed using the signal to noise (S/N) ratio and analysis of variance (ANOVA) for removal of CV from aqueous solutions. The isotherm data were obtained from the experiments performed. The obtained isotherm data were analyzed via the Langmuir, Freundlich and Temkin isotherm models of which the Langmuir isotherm model fitted the best. Thermodynamic parameters such as $\Delta H°$, $\Delta S°$ and $\Delta G°$ were calculated and the results were 18.5 kJ/mol, 0.057 kJ/mol K and –1.514 kJ/mol at 25°C, respectively. The results of this study indicate that almond shells are efficient adsorbents for removing Crystal Violet (CV) from aqueous solutions. The maximum adsorption capacity was found to be 1.075 mg/g on the almond shells. Adsorption kinetics studies showed that adsorption data can be modeled by a pseudo-second-order model. The optimum conditions for the adsorption on almond shells were found to be: adsorbent dosage = 0.5 g, concentration = 4 ppm, pH = 6, shaking speed = 200 rpm and shaking time = 180 min.

Keywords: Almond shells; Crystal violet; Taguchi method; Adsorption isotherm; Thermodynamics

1. Introduction

Many industrial sectors such as paper, textile, paint, food, plastics and leather use huge amounts of dyes with a wide variety of types every year [1]. These sectors release their waste dyes into wastewater streams. Many of these industrial dyes are highly toxic, carcinogenic, mutagenic and allergenic to living organisms [2–5]. Therefore, research for removing industrial dyes from wastewater systems is significant. There are more than 100,000 commercial dyes available, each with a different chemical composition and structure. Dyes are categorized as anionic, cationic and non-ionic depending on the ionic charge of their molecules [6]. Cationic dyes are more toxic than anionic dyes. Within many dyes, crystal violet (CV) dye is a member of the triphenylmethane group and classified as a cationic dye [7]. CV is used in the manufacturing of various products such as pens, printers, biological stains, dermatological agents, veterinary medicine, intestinal parasites, fungus and dyeing of textiles [8,9]. CV is carcinogenic, mutagenic and toxic to mammalian cells. It can cause severe eye irritation and sore sensitization to light. Additionally, it is harmful by inhalation, ingestion and through skin contact [10,11].

There are multiple physical, chemical and biological treatment methods like flocculation, oxidation, reduction, coagulation, precipitation, photolysis, adsorption, membrane separation, bioaccumulation, biodegradation and electrochemical techniques to remove dyes from wastewater systems [12,13]. However, these methods have disadvantages in terms of application cost and effectiveness [9]. Among these methods, adsorption is better for removing dyes with respect to operation cost, simplicity and inactivity of toxic substances [14–21]. There are many types of solid phase adsorbents for removing dyes from water such as agricultural waste, activated carbon, coal, polymers, clay,

---

*Corresponding author.

sand, and magnetic shells. Among these solid phase adsorbents, activated carbon adsorbents are the most common highly effective adsorbents to capture dyes from wastewater, but they are very expensive due to high cost of production [22]. On the other hand, agricultural waste materials like almond, hazelnut, sunflower seeds and peanut shells, palm kernel fibers, chitosan/oil palm ash, rice husk and orange peels are very cheap and abundant [10,23–25].

In this study, we propose almond shells, which are discarded as waste material from the food industry, as an appropriate low-cost adsorbent for removal of CV from aqueous solutions.

To the best of our knowledge, there has been no coinciding study regarding the optimization of experimental conditions by the Taguchi method on adsorption of CV by almond shell.

Optimum adsorption conditions for CV from aqueous solutions were designated as a function of adsorbent dosage, initial concentration, temperature, shaking speed, pH, particle size and contact time. The compositions of almond shells before and after adsorption were characterized by Fourier transform infrared spectroscopy (FTIR). In order to find the best fitting isotherm model, the Langmuir, Freundlich and Temkin isotherms were applied to the data. Moreover, the kinetics, thermodynamics and isotherms of adsorption were discussed.

The Taguchi experimental design was used to define optimum conditions for the maximum removal of the dye from aqueous solutions and reduce overall testing cost and time [26].

2. Material and methods

2.1. Adsorbent

In this study, the almonds were collected from agricultural areas in Elazig, Turkey and dried naturally for one year and then crushed to get smaller pieces of almond shells. These shells were ground and passed through a set of sieves to filter out particles within a certain diameter range. Ultimately, particles of diameter (D_P) in the range of $0.8952 > D_P > 0.137$ mm were obtained and used without any further pretreatment.

2.2. Adsorbate solution

Analytical grade crystal violet was purchased from Sigma-Aldrich. The dye's characteristics and chemical structure are given in Table 1 and Fig. 1, respectively [27]. One liter of 100 ppm stock solution of crystal violet was prepared by dissolving 0.1 grams of the dye with ultra-pure deionized water (UPDIW) (Purelab Flex). A necessary amount was taken from the stock solution and diluted with UPDIW to prepare desired concentrations (2, 4, 6, 8, and 10 ppm). The dye pH was adjusted by using 0.1 M HCl and/or 0.1 M NaOH.

2.3. Crystal violet removal studies

Removal experiments were carried out in 100 mL Erlenmeyer flasks and the volumes of batch reactions were kept

Table 1
The physical characteristics of Crystal Violet

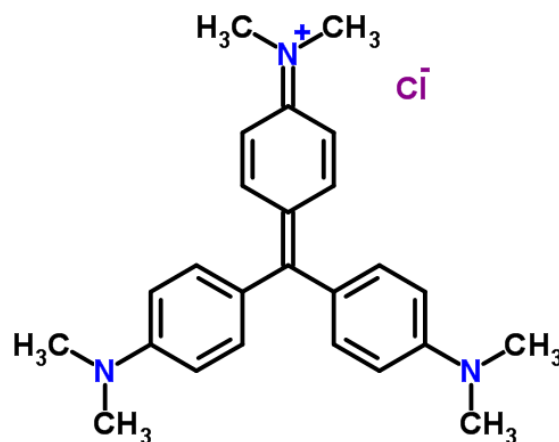| Dye name	Crystal Violet
Abbreviation	CV
Generic name	Basic Violet 3
Chemical name (IUPAC)	Chloride, Hexamethylpararosaniline
Λ_{max}(nm)	584
Color index number	42555
Chemical formula	$C_{25}H_{30}ClN_3$
Molecular weight (g/mol)	407.979

Fig. 1. The chemical structure of Crystal Violet.

at 50 mL. The effects of solution pH (2–10), temperature (20–50°C), contact time (5–180 min), initial concentration (2–10 ppm), adsorbent dosage (0.1–0.5 gram) and shaking speed (150–250 rpm) on the adsorption rate were observed. After each adsorption process, samples were withdrawn at different time intervals. The supernatant was separated from the solutions by utilizing a centrifuge for 5 min at 5000 rpm. The samples at an initial time and each time interval were analyzed using a double beam UV-VIS spectrophotometer at 590 nm (Shimadzu, Model, Japan).

2.4. Taguchi's method of experimental design

Classical experiment design methods are complex and difficult to apply. Moreover, these methods need a large number of experiments with an increasing number of experiment parameters. In order to keep the number of experiments at minimum, the Taguchi method was deemed an appropriate tool [28]. The Taguchi method is an application for designing and analyzing experiments. The major difference between the Taguchi method and conventional experimental designs is that orthogonal arrays are used in the Taguchi design to ensure that the effects of parameters can be reproduced [29]. Another dissimilarity is the signal to noise ratios (S/N) which measure the variability around the desired outcome. There are three forms of S/N ratios, as smaller-the-better, larger-the-better and nominal-the-best

[30]. Smaller-the-better and larger-the-better forms are expressed in Eqs. (1) and (2), respectively.

$$SN_S = -10\log_{10}\left(\frac{1}{n}\sum_{i=1}^{n}Y_i^2\right) \qquad (1)$$

$$SN_L = -10\log_{10}\left(\frac{1}{n}\sum_{i=1}^{n}\frac{1}{Y_i^2}\right) \qquad (2)$$

where SN_S and SN_L are the performance characteristics, n is the number of repetitions under the same experimental conditions, and Y_i is a measured value of the ith experiment [31].

3. Results and discussion

3.1. Effect of optimum adsorbent dosage

The influence of optimum adsorbent dosage was investigated at a constant shaking speed (200 rpm) and temperature (20°C) with varying levels of initial dye concentration (2, 4, 6, 8, and 10 ppm for 24 h). As shown in Fig. 2, the removal percentage of CV increased with the increasing amount of adsorbent. This was due to the fact that availability of active sites (i.e. adsorption area on the surface of almond shells) was positively related to the amount of adsorbent dosage. Moreover, the adsorption capacity was decreasing with the increasing amount of adsorbent dosage and it reached the optimum adsorption value at 0.4 g. This may have been due to aggregation or overlapping of adsorption sites which caused a reduced level of surface area available to dye ions. As seen in Fig. 2, the optimum adsorbent dosage value for adsorption was chosen as 0.4 g and it was used in further experiments.

3.2. Effect of pH on dye adsorption

The effect of the initial pH of the solution on adsorption experiments was analyzed in the range of pH 4–7. The experiments were carried out at a temperature of 20°C, the adsorbent dosage of 0.4 g, initial concentration in the range of 2–10 ppm and shaking speed of 200 rpm for
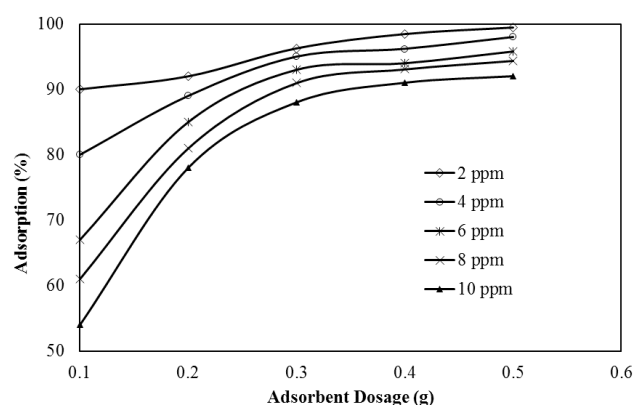
24 h. Additionally, to determine the effects of pH changing with time, additional experiments were carried out with the same experimental conditions and they were constantly monitored for a period of 0–180 min. The effects of pH on CV adsorption for 24 h and different time scales are shown in Figs. 3 and 4, respectively. Based on our results, adsorption of CV onto almond shells increased with increasing solution pH. This may have been due to dye cations and H+ ions competing over the adsorption sites at lower pH values, as suggested in earlier studies [32,33]. Furthermore, the surface of almond shells may have been negatively charged at higher pH levels which would increase the number of dye cations on the surface via electrostatic attraction, as mentioned in former studies [34,35].

3.3. Effect of initial concentration of CV solution

In order to investigate the effects of initial dye concentration on adsorption experiments, the concentration varied in the range of 2–10 ppm at a constant adsorbent dosage of 0.4 g, a temperature of 20°C, and a shaking speed of 200 rpm. As shown in Fig. 5, the removal dye percentage changed with initial concentration, the amount of dye adsorbent on almond shells increased with increasing initial concentration of CV while the percentage of adsorption of the dye decreased with the increasing mass of the adsorbent. This
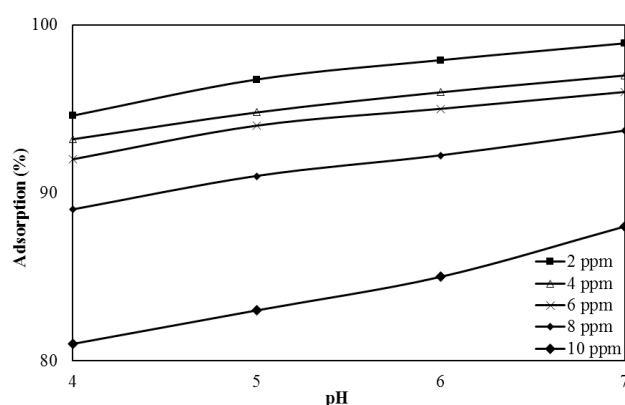
Fig. 3. Effect of initial pH on CV adsorption.
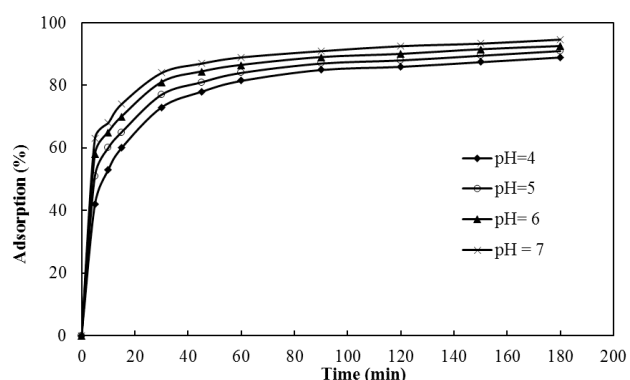
Fig. 2. Effect of adsorbent dosage on CV adsorption.

Fig. 4. Effect of initial pH on CV adsorption for various contact time.

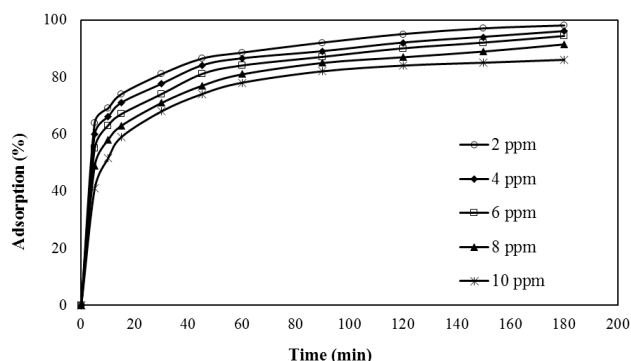Fig. 5. Effect of initial concentration on CV adsorption for various contact time.

Fig. 6. Effect of shaking speed on CV adsorption for various contact time.

may be based on the increasing concentration caused by the increasing driving force between the aqueous and solid phase and the increasing amount of collisions between dye molecules and adsorbent particles [36].

3.4. Effect of shaking speed

The effect of shaking speeds at 150, 175, 200, 225, and 250 rpm were observed while keeping other parameters constant such as the temperature at 20°C, the adsorbent dosage at 0.4 g, the initial concentration at 6 ppm and the natural pH of the solutions. As shown in Fig. 6, the adsorption of the dye increased with the increasing shaking speed. This signifies that while shaking speed was increasing, the thickness of the diffusion layer around almond shells was being reduced [37].

3.5. Effect of temperature

The effects of temperature on adsorption at 20, 30, 40 and 50°C were observed while other parameters were constant such as the adsorbent dosage at 0.4 g, the initial concentration at 6 ppm, and the shaking speed at 200 rpm. The effect of temperature is seen in Fig. 7, while the dye removal percentage increased by increasing the temperature from 20°C to 50°C. This study further suggests that the removal of dye increased with increased temperature, thus the system was identified as endothermic. It may be observed that the increase in temperature led to rising mobility of dye molecules which further led to increasing penetration of adsorbent pores [38,39].

3.6. Effect of particle size

A set of experiments was performed to determine the effects of particle size on dye adsorption. Almond shell particles were separated in the range of 137–892 μm and used in the experiments while other parameters were kept constant, such as the adsorbent dosage at 0.4 g, the initial concentration at 6 ppm, the shaking speed at 200 rpm and the temperature at 20°C. As seen in Fig. 8, dye adsorption on almond shells was increasing with the decreasing particle size of the adsorbent. The adsorbent with finer particle size had higher adsorption capacity than the other with coarse
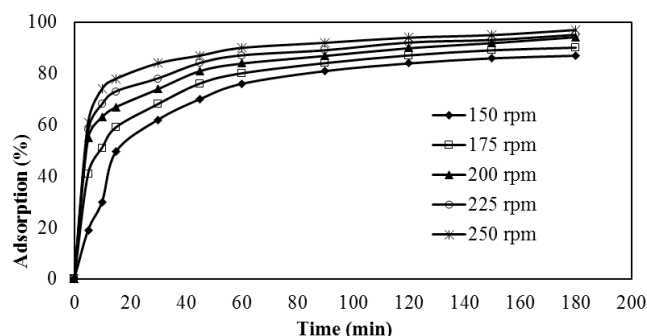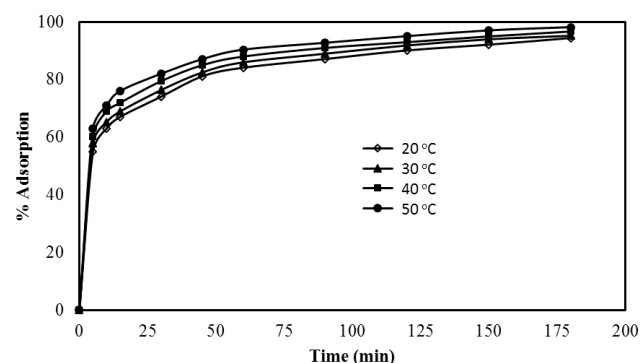

Fig. 7. Effect of temperature on CV adsorption for various contact time.
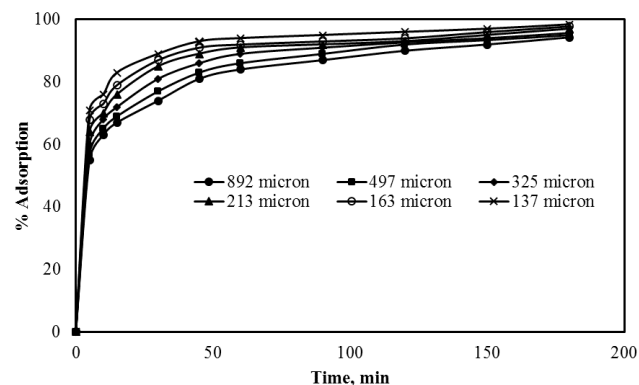
Fig. 8. Effect of particle size on CV adsorption for various contact times.

particle size due to the higher surface area for dye adsorption [40,41].

3.7. Adsorption isotherms

Adsorption equilibrium isotherms have significant value for design and optimization of adsorption systems for removal of dye molecules from aqueous solutions. Estimation of interaction between the adsorbate and the adsorbent could be achieved via these isotherms [42]. In this study, the equilibrium data were analyzed with the Langmuir, Freun-

dlich and Temkin isotherms. The Langmuir isotherm theory suggests that there is monolayer adsorption on a structurally homogeneous outer surface adsorbent and once a dye molecule takes up a site, no other molecules can occupy this place anymore [43]. The Freundlich isotherm model is an empirical expression, which assumes that surface of the adsorbent is heterogeneous, and an exponential distribution of sites and their energies [44]. The Temkin model proposes that heat of adsorption would reduce linearly with rising thickness on the adsorbent [45]. The linear equations of the Langmuir, Freundlich and Temkin models [27] are given by Eqs. (3)–(5), respectively.

$$\frac{1}{q_e} = \frac{1}{q_{max} K_L C_e} + \frac{1}{q_{max}} \tag{3}$$

$$\ln q_e = \ln K_F + \frac{1}{n} \ln C_e \tag{4}$$

$$q_e = B \ln A + B \ln C_e \tag{5}$$

where q_e is the amount of dye adsorbed at equilibrium (mg/g), q_{max} the maximum adsorption capacity after monolayer all covered on the surface (mg/g), K_L is the Langmuir constant related to the energy of adsorption, C_e is the equilibrium concentration of the adsorbate (mg/L), K_F is the Freundlich constant related to adsorption capacity, $1/n$ is the heterogeneity factors related to binding strength, A is a Temkin isotherm constant (L/g), B is related to heat of adsorption (J/mol). The Langmuir, Freundlich and Temkin isotherm correlation coefficients were found to be 0.995, 0.983 and 0.986, respectively. The linear plot of $1/q_e$ vs. $1/C_e$ shows that the adsorption model fits the Langmuir model. The Langmuir constants q_{max} and K_L were determined from the slope and intercepts of the plot and found to be 1.232 and 4.522, respectively.

The essential characteristic of the Langmuir isotherm can be stated with the dimensionless equilibrium parameter (R_L) that is given by Eq. (6).

$$R_L = \frac{1}{1 + K_L C_0} \tag{6}$$

where C_0 is the highest initial dye concentration (mg/L) and K_L is the Langmuir constant. The value of R_L indicates the type of isotherm accordingly:

$R_L > 1$ unfavorable adsorption
$0 < R_L < 1$ favorable adsorption
$R_L = 1$ linear adsorption
$R_L = 0$ irreversible adsorption

The values of R_L were found to be 0.0996, 0.0524, 0.0355, 0.0269 and 0.0216 for initial concentrations of 2, 4, 6, 8 and 10 ppm, respectively, which confirms favorable adsorption of CV on almond shells [46]. The plot of $\ln q_e$ vs. $\ln C_e$ was analyzed to find applicability of the Freundlich isotherm model. The slope ($1/n$) of the plot, which ranges from 0 to 1, represents adsorption level intensity as well as surface heterogeneity. As the value of $1/n$ gets closer to 0, the surface becomes more heterogeneous, whereas, when the value gets closer to 1, it represents a cooperative adsorption. The values of B and A could be calculated from the plot of q_e vs. $\ln C_e$. The Temkin isotherm model suggests that the heat of adsorption of all molecules in the layer decreases linearly with decreasing coverage based on the adsorbent-adsorbate interaction [47].

3.8. Thermodynamic parameters

Increased adsorption of the dye with increased temperature represents that the process was endothermic and it could be explained by thermodynamic parameters such as standard free energy change (ΔG°), enthalpy change (ΔH°) and entropy change (ΔS°). These parameters were calculated using the following equations [48]:

$$K_C = C_{ac}/C_e \tag{7}$$

$$DG° = -RT \ln K_C \tag{8}$$

$$DG° = DH° - TDS° \tag{9}$$

Rearranging Eqs. (8) and (9) to obtain a linear form of the following equation:

$$\ln K_C = \left(\frac{\Delta S°}{R}\right) - \left(\frac{\Delta H°}{RT}\right) \tag{10}$$

It is called the Van't Hoff equation, where, K_C is the equilibrium constant, C_{ac} and C_e are the concentration of dye on the adsorbent and in the solution (mg/L) at equilibrium, respectively. R is the gas constant (8.314 J/mol K) and T is the temperature (K).

The intersection and slope of the linear plot of $\ln K_C$ vs. $1/T$ give ΔS° and ΔH°, respectively and the values were 0.057 kj/mol K for ΔS° and 18.5 kJ/mol for ΔH°. Moreover, ΔG° can be calculated by Eq. (9) for different temperatures such as 298, 303, 313 and 323 K and the values were –1.514, –1.229, –0.659 and –0.089 kJ/mol, respectively. A positive value of ΔH° implies that the nature of adsorption process is endothermic. A positive value of ΔS° indicates analogy of adsorbent and states the increased randomness at solute-solution interface [48]. A negative value of ΔG° remarks that the process is spontaneous and the feasibility of dye adsorption [49].

3.9. Adsorption kinetics

The adsorption kinetic data can be analyzed to determine the dynamics of the adsorption reaction with respect to the order of the rate constant, as kinetic parameters offer significant information for modelling and designing the adsorption process [50]. In order to analyze the adsorption kinetic data, pseudo-first and pseudo-second orders were applied.

A plot of $\log(q_e - q_t)$ vs. t is given in Fig. 9 which shows a linear relationship and q_e and k_1 were calculated from the intercept and slope of the plot [51], respectively.

A plot of t/q_t vs. t (Fig. 10) gives a linear relationship and the slope and intercept of the plots give the value of q_e and k_2 respectively [52]. The results that fit experimental values with pseudo- first and second order model were represented in Table 2. According to data in the table, the correlation coefficients (R^2) of the pseudo-second order model exceeded 0.99 and the calculated q_e values of the

pseudo-second order model were more agreeable with the experimental data than those in the pseudo-first-order model. As a consequence, the adsorption kinetics were represented better with the pseudo-second-order model than with the pseudo-first-order model.

3.10. Adsorption mechanism

The adsorption mechanism cannot be described by the pseudo-first-order and pseudo second order kinetic models, therefore, the kinetic results were examined by utilizing the intra-particle diffusion model [53]. The adsorption mechanism is usually divided into the following steps [54];
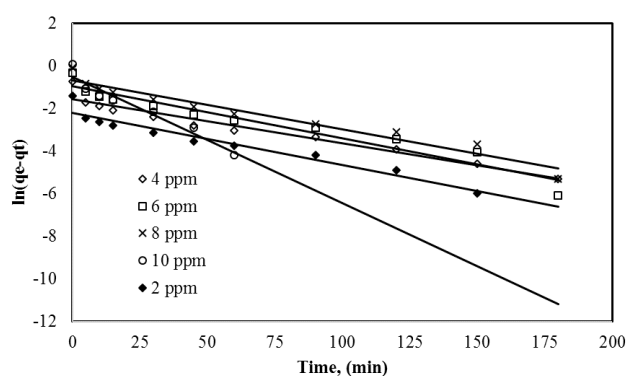

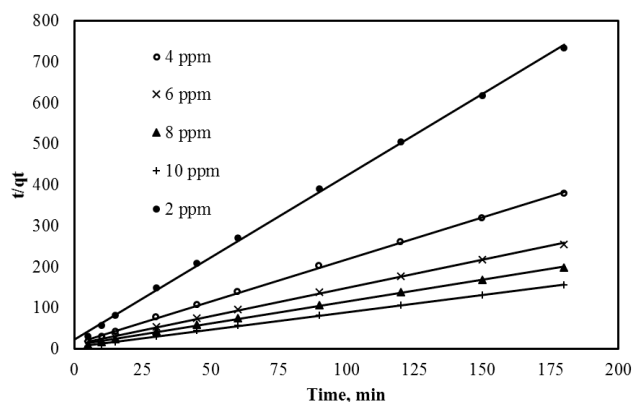Fig. 9. Pseudo first order kinetic for CV on almond shell.

Fig. 10. Pseudo second order kinetic for CV on almond shell.

1. Dye molecules from the liquid solution to boundary layer surrounding the adsorbent (bulk diffusion)
2. Transfer of dye molecules in boundary film to the external surface of sorbent (film diffusion)
3. Transport of the molecules from the surface to intra-particle active sites (intra-particle diffusion)
4. Adsorption of the molecules by the active sites of adsorbent.

The first and the last steps do not involve the rate controlling steps because the first step is not related to the adsorbent and the last step is a quick operation. Therefore, film and intra-particle diffusion are mainly related to the rate controlling steps. The Weber and Morris intra-particle diffusion model is widely used for estimating the rate controlling steps. The intra-particle diffusion constant k_{id} (mg g^{-1} min$^{1/2}$) was described by Eq. (11) [55].

$$q_t = k_{id} t^{1/2} + C \tag{11}$$

where q_t is the amount of adsorbed CV at time t, $t^{1/2}$ is the square root of the time and C is the thickness of the boundary layer. If the plot of q_t vs. $t^{1/2}$ Fig. 11 is a straight line, the mechanism of adsorption process fits the intra-particle diffusion model and the k_{id} and C can be calculated by the slope and intercept of the plot, respectively. In the plot, the first sharp line shows the external surface adsorption also known as the instantaneous adsorption stage. Larger slopes of the first sharp line imply that the adsorption rate is very high at the initial time which depends on the existence of plenty of surface area and active adsorption sites. The second subdued line represents the gradual adsorption stage where the intra-particle diffusion is limiting rate. Lower slopes of the second sharp line indicate that the diffusion of CV molecules on the micropores of adsorbent take a long time due to decreased concentration profile. For some cases, the third subdued line, which is the final equilibrium stage, appears. For this stage, intraparticle diffusion begins to slow down due to very low adsorbate concentration left in the bulk solution [56].

3.11. Fourier transform infrared (FTIR) spectroscopy study

Chemical characterization of the adsorbent surface was accomplished by FTIR analysis. The FTIR spectra of the almond shells before and after dye adsorption were com-

Table 2
Comparison of kinetic parameters for different initial concentration of CV

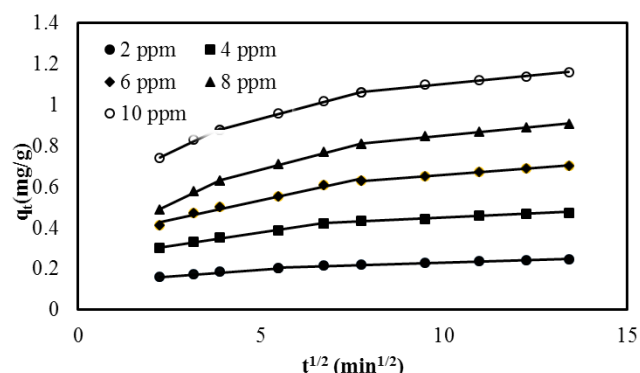| Initial concentration (mg/L)	$q_{e,exp}$ (mg/g)	Pseudo-first-order kinetic model			Pseudo-second-order kinetic model		
		k_1 (1/h)	$q_{e,cal}$ (mg/g)	R^2	k_2 (g/mg h)	$q_{e,cal}$ (mg/g)	R^2
2	0.245	0.0244	0.111	0.9374	0.69	0.25	0.9992
4	0.48	0.0208	0.21	0.9457	0.344	0.486	0.9993
6	0.70725	0.0244	0.38	0.9290	0.197	0.721	0.9989
8	0.915	0.023	0.497	0.9491	0.138	0.936	0.999
10	1.075	0.0594	0.604	0.9394	0.152	1.182	0.9994

Fig. 11. Intra-particle diffusion model for the adsorption of CV onto almond shell.

pared and the results were analyzed. The band at 3419.08 shows the existence of –OH and –NH groups. The peak at 2921.75 represents asymmetric stretches of the –CH group. The band at 1744.24 is associated to stretch vibration of C=O groups [57]. The bands appearing at 1617.89 and 1384.61 are based on stretching vibration of the carbonyl group and C-H deformation vibration [58]. Another three adsorption bands were seen at 1252.27, 1049.06 and 617.07 which could be due to the C-O stretching, sulphonic group and C-S stretching vibration, respectively [59]. The characteristic band at 1744.24 shifted to 1750.57 after CV adsorption. This indicates that there was a chemical inter-action between CV molecules and the carboxylate groups onto the almond shell surface. Moreover, there were other peaks shifting from 3419.08 to 3466.70 cm^{-1} and 1252.27 to 1263.7 cm^{-1}, which showed that the amine and hydroxyl groups were in charge of the CV adsorption on almond shells.

3.12 Comparison of almond shells with other adsorbents

In Table 3, there is a comparison of the maximum crystal violet adsorption capacities of several adsorbents including almond shells. It can be stated that the adsorp-tion capacity of almond shells was lower than those of others. However, almond shells are very cheap and easy to obtain in comparison to other sorbent materials. More-over, almond shells used in this study did not require any pretreatment.

3.13. Taguchi optimization

At the optimum condition, the adsorption capacity of the adsorbent (almond shells) should be as high as possible; hence a larger-the-better S/N ratio was preferred. In order to determine the appropriate orthogonal array, all degrees of the orthogonal array must be evaluated. In this study, five experimental parameters and their five levels were considered; hence, each parameter had four degrees of free-dom, thus making the parameter total 20. Therefore, the L25 orthogonal array was suitable for the experiments [63].

There were five experimental control factors with five levels and L25 orthogonal array are given in Tables 4 and 5, respectively.

Table 3
Comparison of CV adsorption capacity of almond shells to other presented low-cost adsorbents.

Sorbent	q_{max} (mg/g)	Reference
Calotropis procera leaf	4.14	60
Sugarcane dust	3.798	61
Neem sawdust	3.789	62
Almond shell	1.075	This study

Table 4
Experimental parameters and their levels

Parameters		Levels				
		1	2	3	4	5
A	Adsorbent dosage (g)	0.1	0.2	0.3	0.4	0.5
B	Concentration (ppm)	2	4	6	8	10
C	pH	4	5	6	8	10
D	Shaking speed (rpm)	150	175	200	225	250
E	Shaking time (min)	30	60	90	120	180

Table 5
Experimental Taguchi L25 orthogonal array

Experimental number	Parameters and their levels				
	A	B	C	D	E
1	1	1	1	1	1
2	1	2	2	2	2
3	1	3	3	3	3
4	1	4	4	4	4
5	1	5	5	5	5
6	2	1	2	3	4
7	2	2	3	4	5
8	2	3	4	5	1
9	2	4	5	1	2
10	2	5	1	2	3
11	3	1	3	5	2
12	3	2	4	1	3
13	3	3	5	2	4
14	3	4	1	3	5
15	3	5	2	4	1
16	4	1	4	2	5
17	4	2	5	3	1
18	4	3	1	4	2
19	4	4	2	5	3
20	4	5	3	1	4
21	5	1	5	4	3
22	5	2	1	5	4
23	5	3	2	1	5
24	5	4	3	2	1
25	5	5	4	3	2

3.14. Statistical analysis

The collected experimental data were analyzed to calculate the effect of each parameter on the optimization criteria. The calculated means of the S/N ratio and percentage of adsorption for each level of parameters, which was applied to CV adsorption, is shown in Table 6. In order to find the effective parameters and their confidence level on the adsorption of dye, an analysis of variance (ANOVA) was performed [64]. F-test is a useful tool to determine which process parameters have a significant effect in obtaining the maximum adsorption of dye. Table 7 shows the result of the ANOVA for the experiments. The F-value is the ratio of the mean of squared deviations to the mean of squared error for each control factor. Usually, we observe that the greater the F-value is, the larger is the effect on obtaining the maximum adsorption on the adsorbent [65]. From Table 7, it may be seen that the F-value for adsorbent dosage was the highest at 41.82. Therefore, the adsorbent dosage was the most predominant effect on adsorption of CV onto almond shells. In order to get the optimal adsorption performance, larger-the-better performance characteristic in Eq. (2) was used for the adsorption of dye and the obtained values were plotted in Fig. 12. The maximum points in each plot show the best value of the particular parameter. The optimum conditions for the adsorption on almond shells were: adsorbent dosage = 0.5 g, concentration = 4 ppm, pH = 6, shaking speed = 200 rpm and shaking time = 180 min. As a result, there was a logical connection between the experimental data and the statistical analysis data.

4. Conclusion

In this study, there were three important outcomes: the optimum condition was obtained by the Taguchi method, adsorption rate changed with changing experimental conditions, and a new adsorbent was discovered for crystal vio-

Table 7
Analysis of variance (ANOVA) for SN ratio for crystal violet removal

Parameters	Sum of Squares	Degrees of Freedom	Mean Square	F-value
A (Adsorbent dosage)	25.49	4	6.37	41.82
B (Concentration)	4.1	1	4.1	26.91
C (pH)	1.75	4	0.44	2.88
D (Shaking speed)	0.32	4	0.081	0.53
E (Shaking time)	1.73	1	1.73	11.38
Residual	1.52	10	0.15	

Table 6
Parameters, their values corresponding to their levels and SN values

| Adsorbent dosage	Concentration	pH	Shaking speed	Shaking time	% Adsorption	S/N	Mean
0.1	2	4	150	30	38	31.5957	38
0.1	4	5	175	60	54	34.6479	54
0.1	6	6	200	90	49	33.8039	49
0.1	8	8	225	120	40	32.0412	40
0.1	10	10	250	180	48	33.6248	48
0.2	2	5	200	120	81	38.1697	81
0.2	4	6	225	180	92	39.2758	92
0.2	6	8	250	30	64	36.1236	64
0.2	8	10	150	60	63	35.9868	63
0.2	10	4	175	90	43	32.6694	43
0.3	2	6	250	60	86	38.6900	86
0.3	4	8	150	90	79	37.9525	79
0.3	6	10	175	120	85	38.5884	85
0.3	8	4	200	180	75	37.5012	75
0.3	10	5	225	30	60	35.5630	60
0.4	2	8	175	180	99	39.9127	99
0.4	4	10	200	30	91	39.1808	91
0.4	6	4	225	60	85	38.5884	85
0.4	8	5	250	90	88	38.8897	88
0.4	10	6	150	120	79	37.9525	79
0.5	2	10	225	90	98	39.8245	98
0.5	4	4	250	120	97	39.7354	97
0.5	6	5	150	180	97	39.7354	97
0.5	8	6	175	30	88	38.8897	88
0.5	10	8	200	60	77	37.7298	77
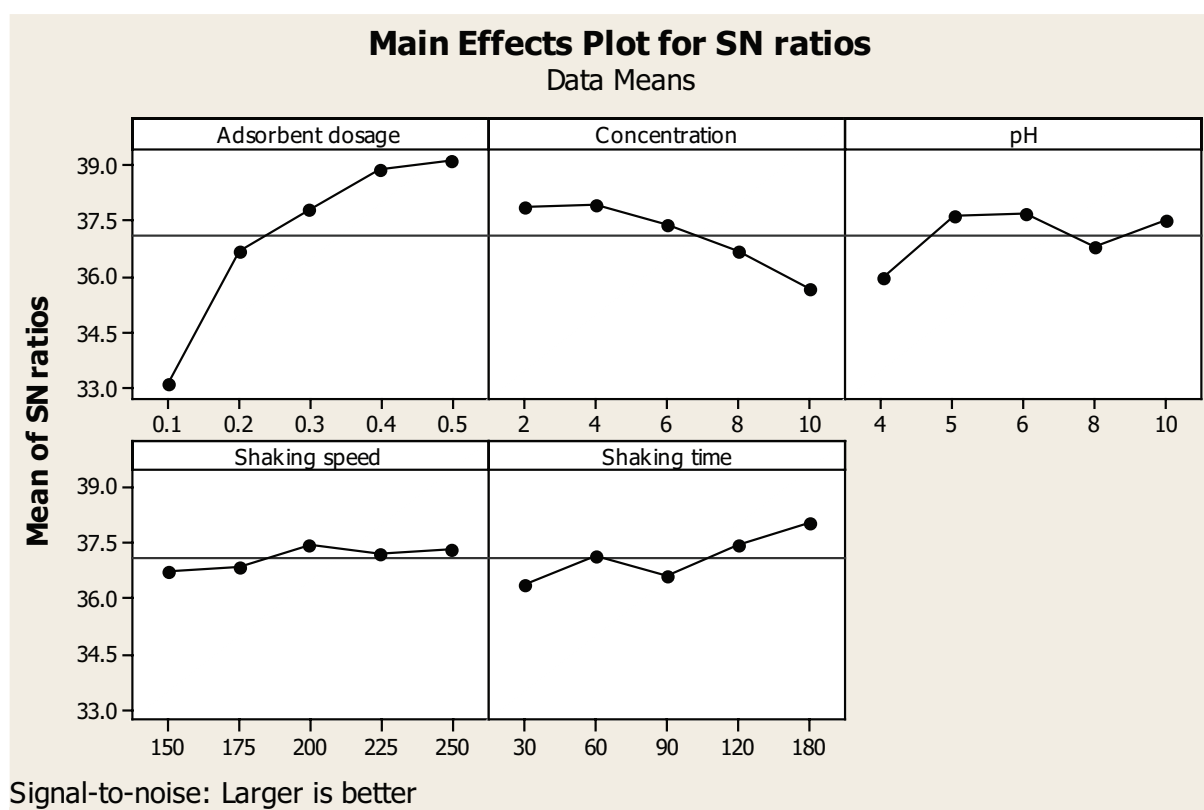
Fig. 12. Effects of the parameters on S/N ratio.

let. The adsorption experiment implied that almond shells may be used for effective removal of CV from aqueous solutions. Since almond shells are an abundant waste material that needs no further pretreatment, the adsorbent is economically viable for removal of CV from aqueous solutions. The amount of dye adsorbed on almond shells was found to increase with increasing amounts of the adsorbent, pH, initial concentration, shaking speed and temperature, but decrease with increasing particle sizes of the adsorbent. The adsorption followed pseudo-second-order kinetic equations. The experimental equilibrium data from batch experiments fit well into the Langmuir adsorption isotherm model. The calculated thermodynamic parameters of $\Delta H°$, $\Delta G°$ and $\Delta S°$ indicated that the adsorption on almond shells was endothermic, spontaneous and there was increased randomness at the solid/solution interface. Moreover, the Taguchi method was applied to find the optimum removal condition through 25 experiments. The influencing scope of the controllable factors of CV removal in descending order was A>B>E>C>D. Therefore, the adsorbent dosage was the most influential factor and the shaking speed was the least influencing factor.

The contribution of the paper is twofold. First, almond shells are an economical option in removing CV from aqueous solutions. Second, adsorption of CV onto almond shells changes with the amount of the adsorbent, pH of solutions, initial concentration, shaking speed, temperature and particle size. Almond shells, which are an agricultural waste, could be used effectively for removal of basic dyes in industrial waste streams.

References

[1] H. Shayesteh, A. Rahbar-Kelishami, R. Norouzbeigi, Adsorption of malachite green and crystal violet cationic dyes from aqueous solution using pumice stone as a low-cost adsorbent: kinetic, equilibrium, and thermodynamic studies, Desal. Water Treat., 57 (2016) 12822–12831.
[2] A.M. Aljeboree, A.F. Alkaim, A.H. Al-Dujaili, Adsorption isotherm, kinetic modeling and thermodynamics of crystal violet dye on coconut husk-based activated carbon, Desal. Water Treat., 53 (2015) 3656–3667.
[3] A. Bazzo, M.A. Adebayo, S.L.P. Dias, E.C. Lima, J.C.P. Vaghetti, E.R. de Oliveira, A.J.B. Leite, F.A. Pavan, Avocado seed powder: characterization and its application for crystal violet dye removal from aqueous solutions, Desal. Water Treat., 57 (2016) 15873–15888.
[4] M. Naushad, A. Mittal, M. Rathore, V. Gupta, Ion-exchange kinetic studies for Cd(II), Co(II), Cu(II), and Pb(II) metal ions over a composite cation exchanger, Desal. Water Treat., 54 (2015) 2883–2890.
[5] A. Mittal, Retrospection of Bhopal gas tragedy, Toxicol. Environ. Chem., 98 (2016) 1079–1083.
[6] M.M.R. Khan, M.W. Rahman, H.R. Ong, A.B. Ismail, C.K. Cheng, Tea dust as a potential low-cost adsorbent for the removal of crystal violet from aqueous solution, Desal. Water Treat., 57 (2016) 14728–14738.

[7] S. Neupane, S.T. Ramesh, R. Gandhimathi, P.V. Nidheesh, Pineapple leaf (Ananas comosus) powder as a biosorbent for the removal of crystal violet from aqueous solution, Desal. Water Treat., 54 (2015) 2041–2054.

[8] L.B.L. Lim, N. Priyantha, T. Zehra, C.W. Then, C.M. Chan, Adsorption of crystal violet dye from aqueous solution onto chemically treated Artocarpus odoratissimus skin: equilibrium, thermodynamics, and kinetics studies, Desal. Water Treat., 57 (2016) 10246–10260.

[9] H. Yang, D. Zhou, Z. Chang, L. Zhang, Adsorption of crystal violet onto amino silica: optimization, equilibrium, and kinetic studies, Desal. Water Treat., 52 (2014) 6113–6121.

[10] A. Saeed, M. Sharif, M. Iqbal, Application potential of grapefruit peel as dye sorbent: Kinetics, equilibrium and mechanism of crystal violet adsorption, J. Hazard. Mater., 179 (2010) 564–572.

[11] K.P. Singh, S. Gupta, A.K. Singh, S. Sinha, Optimizing adsorption of crystal violet dye from water by magnetic nanocomposite using response surface modeling approach, J. Hazard. Mater., 186 (2011) 1462–1473.

[12] A. Mittal, L. Kurup, Column operations for the removal and recovery of a hazardous dye "Acid Red - 27" from aqueous solutions, using waste materials – bottom ash and de-oiled soya, Ecol. Env. & Cons., 13 (2006) 181–186.

[13] S. Kaur, S. Rani, R.K. Mahajan, Adsorption of dye crystal violet onto surface-modified Eichhornia crassipes, Desal. Water Treat., 53 (2015) 1957–1969.

[14] A. Mittal, M. Teotia, R.K. Soni, J. Mittal, Applications of egg shell and egg shell membrane as adsorbents: A review, J. Mol. Liq., 223 (2016) 376–387.

[15] A. Mittal, R. Ahmad, I. Hasan, Iron oxide-impregnated dextrin nanocomposite: synthesis and its application for the biosorption of Cr(VI) ions from aqueous solution, Desal. Water Treat., 57 (2016) 15133–15145.

[16] A. Mittal, R. Ahmad, I. Hasan, Biosorption of Pb^{2+}, Ni^{2+} and Cu^{2+} ions from aqueous solutions by L-cystein-modified montmorillonite-immobilized alginate nanocomposite, Desal. Water Treat., 57 (2016) 17790–17807.

[17] A. Mittal, R. Ahmad, I. Hasan, Poly (methyl methacrylate)-grafted alginate/Fe_3O_4 nanocomposite: synthesis and its application for the removal of heavy metal ions, Desal. Water Treat., 57 (2016) 19820–19833.

[18] A. Mittal, M. Naushad, G. Sharma, Z.A. ALothman, S.M. Wabaidur, M. Alam, Fabrication of MWCNTs/ThO_2 nanocomposite and its adsorption behavior for the removal of Pb(II) metal from aqueous medium, Desal. Water Treat., 57 (2016) 21863–21869.

[19] R. Ahmad, I. Hasan, A. Mittal, Adsorption of Cr (VI) and Cd (II) on chitosan grafted polyaniline-OMMT nanocomposite: isotherms, kinetics and thermodynamics studies, Desal. Water Treat., 58 (2017) 144–153.

[20] X. Ren, W. Xiao, R. Zhang, Y. Shang, R. Han, Adsorption of crystal violet from aqueous solution by chemically modified phoenix tree leaves in batch mode, Desal. Water Treat., 53 (2015) 1324–1334.

[21] M.K. Satapathy, P. Das, Assessment on the modelling of the kinetic parameter for the removal of crystal violet dye using Ag-soil nanocomposite: linear and non-linear analysis, Desal. Water Treat., 57 (2016) 4073–4080.

[22] I.A.W. Tan, B.H. Hameed, Removal of crystal violet dye from aqueous solutions using rubber (hevea brasillensis) seed shell-based biosorbent, Desal. Water Treat., 48 (2012) 174–181.

[23] G. Sharma, M. Naushad, D. Pathania, A. Mittal, G.E. El-desoky, Modification of Hibiscus cannabinus fiber by graft copolymerization: application for dye removal, Desal. Water Treat., 54 (2015) 3114–3121.

[24] S.K. Sharma, ed. Green Chemistry for Dyes Removal from Waste Water: Research Trends and Applications, John Wiley & Sons, New Jersey (USA), 2015, pp. 409–457.

[25] B.K. Suyamboo, R. Srikrishnaperumal, Biosorption of crystal violet onto cyperus rotundus in batch system: kinetic and equilibrium modeling, Desal. Water Treat., 52 (2014) 3535–3546.

[26] M.P. Elizalde-Gonzalez, L.E. Garcia-Diaz, Application of a Taguchi L16 orthogonal array for optimizing the removal of Acid Orange 8 using carbon with a low specific surface area, Chem. Eng. J., 163 (2010) 55–61.

[27] R. Ahmad, Studies on adsorption of crystal violet dye from aqueous solution onto coniferous pinus bark powder (CPBP), J. Hazard. Mater., 171 (2009) 767–773.

[28] E. Bagci, B. Ozcelik, Analysis of temperature changes on the twist drill under different drilling conditions based on Taguchi method during dry drilling of Al 7075-T651, J. Adv. Manufac. Technol., 29 (2006) 629–636.

[29] V.C. Srivastava, I.D. Mall, I.M. Mishra, Optimization of parameters for adsorption of metal ions onto rice husk ash using Taguchi's experimental design methodology, Chem. Eng. J., 140 (2008) 136–144.

[30] A.B. Engin, Ö. Özdemir, M. Turan, A.Z. Turan, Color removal from textile dyebath effluents in a zeolite fixed bed reactor: Determination of optimum process conditions using Taguchi method, J. Hazard. Mater., 159 (2008) 348–353.

[31] H.Y. Yen, C.P. Lin, Adsorption of Cd(II) from wastewater using spent coffee grounds by Taguchi optimization, Desal. Water Treat., 57 (2016) 11154–11161.

[32] P. Monash, G. Pugazhenthi, Adsorption of crystal violet dye from aqueous solution using mesoporous materials synthesized at room temperature, Adsorption, 15 (2009) 390–405.

[33] L.S. Oliveira, A.S. Franca, T.M. Alves, S.D.F. Rocha, Evaluation of untreated coffee husks as potential biosorbents for treatment of dye contaminated waters, J. Hazard. Mater., 155 (2008) 507–512.

[34] V. Ponnusami, V. Gunasekar, S.N. Srivastava, Kinetics of methylene blue removal from aqueous solution using gulmohar (Delonix regia) plant leaf powder: Multivariate regression analysis, J. Hazard. Mater., 169 (2009) 119–127.

[35] H.B. Senturk, D. Ozdes, C. Duran, Biosorption of Rhodamine 6G from aqueous solutions onto almond shell (Prunus dulcis) as a low cost biosorbent, Desalination, 252 (2010) 81–87.

[36] I.A.W. Tan, A.L. Ahmad, B.H. Hameed, Adsorption isotherms, kinetics, thermodynamics and desorption studies of 2,4,6-trichlorophenol on oil palm empty fruit bunch-based activated carbon, J. Hazard. Mater., 164 (2009) 473–482.

[37] B.K. Nandi, A. Goswami, M.K. Purkait, Removal of cationic dyes from aqueous solutions by kaolin: Kinetic and equilibrium studies, Appl. Clay Sci., 42 (2009) 583–590.

[38] C.A.P. Almeida, N.A. Debacher, A.J. Downs, L. Cottet, C.A.D. Mello, Removal of methylene blue from colored effluents by adsorption on montmorillonite clay, J. Colloid Interface Sci., 332 (2009) 46–53.

[39] S. Senthilkumaar, P. Kalaamani, C.V. Subburaam, Liquid phase adsorption of Crystal violet onto activated carbons derived from male flowers of coconut tree, J. Hazard. Mater., 136 (2006) 800–808.

[40] S. Çoruh, F. Geyikçi, E. Kiliç, U. Çoruh, The use of NARX neural network for modeling of adsorption of zinc ions using activated almond shell as a potential biosorbent, Bioresour. Technol., 151 (2014) 406–410.

[41] S. Babel, T.A. Kurniawan, Low-cost adsorbents for heavy metals uptake from contaminated water: a review, J. Hazard. Mater., 97 (2003) 219–243.

[42] R. Kumar, R. Ahmad, Biosorption of hazardous crystal violet dye from aqueous solution onto treated ginger waste (TGW), Desalination, 265 (2011) 112–118.

[43] F. Doulati Ardejani, K. Badii, N.Y. Limaee, S.Z. Shafaei, A.R. Mirhabibi, Adsorption of Direct Red 80 dye from aqueous solution onto almond shells: Effect of pH, initial concentration and shell type, J. Hazard. Mater., 151 (2008) 730–737.

[44] Y. Bulut, Z. Tez, Adsorption studies on ground shells of hazelnut and almond, J. Hazard. Mater., 149 (2007) 35–41.

[45] T. Aysu, M.M. Küçük, Removal of crystal violet and methylene blue from aqueous solutions by activated carbon prepared from Ferula orientalis, Int. J. Environ. Sci. Technol., 12 (2014) 2273–2284.

[46] K.M. Parida, A.C. Pradhan, Removal of phenolic compounds from aqueous solutions by adsorption onto manganese nodule leached residue, J. Hazard. Mater., 173 (2010) 758–764.

[47] G.O. El-Sayed, Removal of methylene blue and crystal violet from aqueous solutions by palm kernel fiber, Desalination, 272 (2011) 225–232.

[48] N. Ertugay, Basic Violet 10 (BV10) removal from aqueous solutions using sawdust of *Swietenia mahagoni* (Mahogany trees): adsorbent characterization, adsorption isotherm, kinetics, and thermodynamic studies, Desal. Water Treat., 57 (2016) 12335–12349.

[49] O. Gercel, H.F. Gercel, A.S. Koparal, U.B. Ogutveren, Removal of disperse dye from aqueous solution by novel adsorbent prepared from biomass plant material, J. Hazard. Mater., 160 (2008) 668–674.

[50] C. Varlikli, V. Bekiari, M. Kus, N. Boduroglu, I. Oner, P. Lianos, G. Lyberatos, S. Icli, Adsorption of dyes on Sahara desert sand, J. Hazard. Mater., 170 (2009) 27–34.

[51] B.H. Hameed, Equilibrium and kinetic studies of methyl violet sorption by agricultural waste, J. Hazard. Mater., 154 (2008) 204–212.

[52] F. Akbal, Adsorption of basic dyes from aqueous solution onto pumice powder, J. Colloid Interface Sci., 286 (2005) 455–458.

[53] O. Gercel, A. Ozcan, A.S. Ozcan, H.F. Gercel, Preparation of activated carbon from a renewable bio-plant of Euphorbia rigida by H_2SO_4 activation and its adsorption behavior in aqueous solutions, Appl. Surf. Sci., 253 (2007) 4843–4852.

[54] Y. Li, Q. Du, X. Wang, P. Zhang, D. Wang, Z. Wang, Y. Xia, Removal of lead from aqueous solution by activated carbon prepared from Enteromorpha prolifera by zinc chloride activation, J. Hazard. Mater., 183 (2010) 583–589.

[55] L. Wang, J. Zhang, R. Zhao, Y. Li, C. Li, C. Zhang, Adsorption of Pb(II) on activated carbon prepared from Polygonum orientale Linn.: Kinetics, isotherms, pH, and ionic strength studies, Bioresour. Technol., 101 (2010) 5808–5814.

[56] F.C. Wu, R.L. Tseng, R.S. Juang, Comparisons of porous and adsorption properties of carbons activated by steam and KOH, J. Colloid Interface Sci., 283 (2005) 49–56.

[57] B.N. Estevinho, E. Ribeiro, A. Alves, L. Santos, A preliminary feasibility study for pentachlorophenol column sorption by almond shell residues, Chem. Eng. J., 136 (2008) 188–194.

[58] K. Saeed, M. Ishaq, S. Sultan, I. Ahmad, Removal of methyl violet 2-B from aqueous solutions using untreated and magnetite-impregnated almond shell as adsorbents, Desal. Water Treat., 57(29) (2016) 13484–13493.

[59] R. Ahmad, R. Kumar, Adsorption studies of hazardous malachite green onto treated ginger waste, J. Environ. Manage., 91 (2010) 1032–1038.

[60] H. Ali, S.K. Muhammad, Biosorption of crystal violet from water on leaf biomass of Calotropis procera, J. Environ. Sci. Technol., 1 (2008) 143–150.

[61] M.K. Singh, S.D. Khattri, Colour removal from dye wastewater using sugar cane dust as an adsorbent, Adsorpt. Sci. Technol., 17 (1999) 269–282.

[62] S.D. Khattri, M.K. Singh, Colour removal from synthetic dye wastewater using a bioadsorbent, Adsorption, 120 (2000) 283–294.

[63] A. Kundu, B. SenGupta, M.A. Hashim, G. Redzwan, Taguchi optimisation approach for chromium removal in a rotating packed bed contractor, J. Taiwan Inst. Chem. Eng., 57 (2015) 91–97.

[64] F. Toprak, B. Armagan, A. Cakici, Systematic approach for the optimal process conditions of Reactive Red 198 adsorption by pistachio nut shell using Taguchi method, Desalin. Water Treat., 48 (2012) 96–105.

[65] T. Mohammadi, M.A. Safavi, Application of Taguchi method in optimization of desalination by vacuum membrane distillation, Desalination, 249 (2009) 83–89.